

Enhancement to Fusion Reactivity in Sheared Flows

Henry Fetsch* and Nathaniel J. Fisch

Department of Astrophysical Sciences, Princeton University, Princeton, NJ

(Dated: October 7, 2024)

Sheared flow increases the reactivity of fusion plasma. In unmagnetized DT plasma with flow gradients comparable to the mean free path of reacting ions, reactivity can be more than doubled. Neutron spectra are modified, helping to explain anomalous observations. The reactivity enhancement is particularly relevant in inertial confinement fusion (ICF), where it allows turbulent kinetic energy to contribute to the fusion burn even before thermalizing. In high-yield ICF experiments, the effect is most pronounced before bang time, suggesting a new mechanism for fast ignition.

Introduction – The reactivity of fusion plasma is primarily determined by a small number of high-energy ions in the tail of the distribution function, whose mean free paths are many times longer than those of thermal ions. Even when a hydrodynamic description is appropriate for thermal particles, the tail of the distribution often demands a kinetic treatment. In such cases, fusion reactivity $\langle\sigma v\rangle$ becomes a nonlocal functional of fluid properties within a few fast-ion mean free paths. In inertial confinement fusion (ICF) experiments, this leads to a substantial reduction in reactivity within the Knudsen layer, where fast ions are lost from the hot fuel [1–3]. Diffusion, species separation, and thermal decoupling also tend to suppress reactivity [4–9] (with some caveats [6, 10, 11]), while colliding shocks [12] and alpha-particle heating [13] tend to enhance it. Historically, ICF simulations have overpredicted fusion yields [4, 14, 15] and incorrectly predicted neutron spectra [16, 17]. A major effort is now underway to explain these discrepancies, with kinetic effects playing an important role [5, 12, 16–22].

Surprisingly, the effect of inhomogeneous flow on fast ions has so far not been considered. In this Letter, we show that sheared flow drives a large enhancement in reactivity, exceeding a factor of two near strong gradients. Inhomogeneous flow can, of course, modify reactivity by compressing and heating patches of fluid, but, remarkably, even solenoidal flow enhances reactivity through the nonlocal effect of fast ions. The flow can be structured or turbulent, provided that it is sheared on length scales comparable to the fast-ion mean free path. ICF produces the exotic conditions under which this effect can be very large. In both laser-driven [23, 24] and z-pinch [25–27] experiments, a substantial fraction of energy at peak compression resides in turbulent flows, sometimes exceeding the ion thermal energy, and flow gradients are comparable to the ion mean free path [21, 22]. Turbulence is generally deleterious in fusion systems [23, 28–32]; in ICF specifically, turbulent mixing is a major cause of underperformance [33, 34]. We show, however, that turbulence can augment, rather than suppress, reactivity if mixing is mitigated and gradients are strong. In some cases, driving flow is more efficient (per unit energy) than direct heating. In ignition experiments, the enhancement is largest before the fuel is fully compressed. If energy

is left in turbulent motion until just before bang time, as some work has found to be advantageous [35–37], this can be leveraged into an efficient fast-ignition scheme.

The identification of a salutary effect may appear inconsistent with the experimental fact that ICF experiments have regularly underperformed relative to simulations. There is in reality no contradiction; deleterious effects have simply proven larger to date. The balance shifts in larger implosions because the sheared-flow enhancement scales with hotspot volume while Knudsen-layer effects scale with surface area [10]. The kinetic effects of shear help to explain puzzling neutron spectra that appear in ICF experiments and cannot be explained by purely hydrodynamic models [4, 7, 16, 38]. The effect can be understood simply in physical terms as follows.

Physical picture – Consider, as sketched in Fig. 1, a fluid flowing in the x direction and sheared in the z direction. The distribution function at each point is approximately a drifting Maxwellian. A particle sampled from the thermal bulk at z_1 ends up closer to the tail if it reaches z_0 without colliding. For a thermal particle sampled at z_2 , the effect is more pronounced. Some particles will have smaller velocities in their new frame, but the overall effect is to broaden the tail. Neglecting slowing by electrons, the mean free path λ for fast ions scales as $\lambda \propto w^4$, where w is the velocity in the local fluid frame, so faster ions communicate further across the flow gradient. For thermal particles, this effect is well known – it is the origin of viscosity in weakly coupled plasma – but fast particles travel beyond viscous length scales, potentially crossing large flow differentials.

If fluid properties vary on a length scale L , then a useful figure is the Knudsen number $\text{Kn} \doteq \lambda_{\text{th}}/L$, where λ_{th} is the mean free path of a thermal ion. For Maxwellian ions, the reaction rate is peaked at $v_* \propto v_{\text{th}}(E_G/T)^{1/6}$, where the Gamow energy E_G gives the energy scale of the Coulomb barrier, T is the temperature (in units of energy), and v_{th} is the thermal velocity. In many cases, $v_* \gg v_{\text{th}}$. Because most reacting particles have velocities near v_* , their mean free paths λ are much longer than λ_{th} . The ‘Gamow-Knudsen’ number $\text{Gk} \doteq \lambda/L = (v_*/v_{\text{th}})^4 \text{Kn}$ of McDevitt *et al.* thus better captures the effect of gradients on reactivity [1, 10].

When ions cross a flow gradient, they attain some

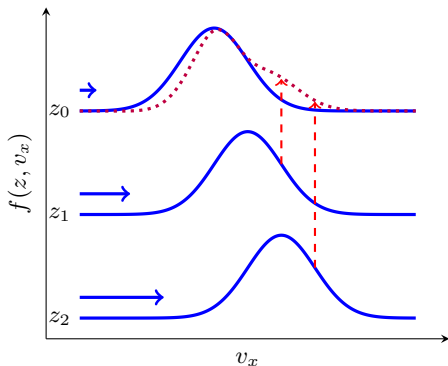


Figure 1: Fast particles crossing a flow gradient perturb the distribution, particularly on the tail.

drift velocity in their new frame; we show here that even a small drift has a large effect on reactivity. Consider a one-dimensional Maxwellian distribution of ions with thermal velocity v_{th} reacting with some stationary background species. Suppose that the fusion power P is roughly proportional to the number of particles at $v_* \gg v_{\text{th}}$ (this is a reasonable estimate for strongly resonant reactions, while for nonresonant reactions it is merely illustrative), so in equilibrium $P^{(\text{eq})} \propto \exp\{-\frac{1}{2}v_*^2/v_{\text{th}}^2\}$. Suppose that we impart to the ions a drift velocity $u \ll v_{\text{th}}\sqrt{v_{\text{th}}/v_*}$. The fusion power is now approximately $P^{(\text{drift})} \propto \exp(-\frac{1}{2}v_*^2/v_{\text{th}}^2 + v_*u/v_{\text{th}}^2)$. The drift energy could instead have been used for heating. If the drifting ions are one quarter of total particles, heating produces a new thermal velocity v'_{th} such that $v'^2_{\text{th}} = v^2_{\text{th}} + \frac{1}{12}u^2$, yielding fusion power $P^{(\text{heat})} \propto \exp(-\frac{1}{2}v_*^2/v_{\text{th}}^2 + \frac{1}{24}v_*^2u^2/v_{\text{th}}^4)$. Denoting by Φ the enhancement factor relative to $P^{(\text{eq})}$, we have

$$\Phi^{(\text{drift})} \sim e^\gamma \quad \text{and} \quad \Phi^{(\text{heat})} \sim e^{\gamma^2/24}, \quad (1)$$

where $\gamma \doteq v_*u/v_{\text{th}}^2$ is the single parameter governing the size of the effect. For $\gamma \gtrsim 1$, fusion power is multiplied manifold even though u is small. For $\gamma < 24$, energy is better spent on drift than on heating. In their general, qualitative form, these conclusions are well known. Beam-target fusion offers a high reaction rate [39, 40], but with low efficiency since most beam ions scatter before fusing. Anisotropic [41] and bimaxwellian [42] distributions increase reaction rates, but energy must be expended to keep such distributions out of equilibrium, which is often prohibitive from an efficiency standpoint [43]. Flow shear obviates this limitation by producing a drifting population of fast ions while barely affecting the thermal bulk.

Kinetic model – To isolate the effect of flow shear, we consider uniform, planar x -directed flows separated by a transition layer of width L at $z = 0$. Away from this

layer, the flow field \mathbf{u} is given by

$$\mathbf{u}(z) = \begin{cases} u_0 \hat{\mathbf{x}} & z \ll L \\ 0 & z \gg L \end{cases} \quad (2)$$

where u_0 is a constant. We first consider regimes in which

$$\text{Kn} \ll 1 \ll \text{Gk}, \quad (3)$$

permitting a hydrodynamic description: thermal particles, which are responsible for the majority of viscous dissipation, have short mean free paths. On the other hand, particles near the Gamow peak travel far beyond the layer before scattering. If we are exclusively interested in the transport of energetic particles, we can treat the layer as a point discontinuity. In the numerical work below, we will relax this assumption to consider systems in which the scale separation (3) is not so large.

For simplicity, we consider a single ion species with mass m , uniform density n , and uniform temperature T . Electrons form a neutralizing background. The distribution function f evolves according to

$$\frac{\partial f}{\partial t} + \mathbf{v} \cdot \nabla f + \mathbf{a} \cdot \frac{\partial f}{\partial \mathbf{v}} = \mathcal{C}[f, f], \quad (4)$$

where \mathbf{v} is the velocity in the laboratory frame, \mathbf{a} is the net acceleration, and \mathcal{C} is a bilinear collision operator.

Let $\mathbf{w} \doteq \mathbf{v} - \mathbf{u}$ be the peculiar velocity and $v_{\text{th}} \doteq (T/m)^{1/2}$ be the thermal velocity. By (3), the bulk of the distribution is approximately a Maxwellian f_M , while the tail may deviate significantly. We approximate collisions as occurring between test particles and a thermal background, adopting a Bhatnagar-Gross-Krook (BGK) operator, *viz.* $\mathcal{C} = -\nu_{\text{ii}}(f - f_M)$ where $\nu_{\text{ii}} = \nu_0$ for $w \leq v_{\text{th}}$, $\nu_{\text{ii}} = \nu_0(v_{\text{th}}/w)^3$ for $w > v_{\text{th}}$, and ν_0 is a constant. We finally assume steady state ($\partial_t f = 0$) and that all spatial variation is in the z direction. Treating the shear layer as a step function, the solution is

$$f(z > 0) \sim \begin{cases} \frac{\hat{f}}{(2\pi)^{3/2}v_{\text{th}}^3} \left[e^{-\frac{z\nu_{\text{ii}}}{w}} \exp\left\{-\frac{|\mathbf{w} - u_0\hat{\mathbf{x}}|^2}{2v_{\text{th}}^2}\right\} \right. \\ \left. + \left(1 - e^{-\frac{z\nu_{\text{ii}}}{w}}\right) \exp\left\{-\frac{|\mathbf{w}|^2}{2v_{\text{th}}^2}\right\} \right] & w_z > 0, \\ \frac{1}{(2\pi)^{3/2}v_{\text{th}}^3} \exp\left\{-\frac{|\mathbf{w}|^2}{2v_{\text{th}}^2}\right\} & w_z \leq 0, \end{cases} \quad (5)$$

where \hat{f} is a normalization factor applied to conserve density. The distribution for $z < 0$ is obtained by reversing signs and shifting velocities by \mathbf{u} .

Fusion reactivity – For a single species, reactivity is

$$\langle \sigma v \rangle = \frac{1}{2}v_{\text{th}} \iint d^3w d^3w' \sqrt{2}p\sigma(p)f(\mathbf{w})f(\mathbf{w}'), \quad (6)$$

where σ is the fusion cross section and $p \doteq (\mathbf{w} - \mathbf{w}')/\sqrt{2}v_{\text{th}}$ is the normalized relative velocity. Assuming a constant S-factor and no resonances,

σ can be approximated by

$$\sigma(p) = \frac{A}{v_{\text{th}}^2 p^2} e^{-b/p}, \quad (7)$$

where A and b are constants (note $b \propto v_{\text{th}}^{-1}$). Physically, b represents the height of the Coulomb barrier relative to the thermal energy ($b^2 \propto E_G/T$). In general, fusion reactions are classically forbidden and require quantum tunneling; in other words, b is large. For DD reactions at 3 keV, for example, $b \approx 26$ [44]. When $b \gg 1$, the integrand is sharply peaked, allowing (6) to be evaluated by steepest descent. We define the enhancement factor Φ to leading order in b by

$$\langle \sigma v \rangle \sim \sqrt{\frac{2}{3}} \frac{Ab^{1/3}}{v_{\text{th}}} e^{-\frac{3}{2}b^{2/3}} \Phi \quad (8)$$

so that $\Phi = 1$ for Maxwellian distributions. Starting from (5) and making the approximation that every fusion reaction involves a fast and a slow particle, where fast and slow mean that $z\nu_0/w^4 \ll 1$ and $z\nu_0/w^4 \gg 1$ respectively, we have

$$\Phi \sim \frac{1}{2} + \frac{\iint \frac{d^3 p d^3 s}{(2\pi)^3} \frac{e^{-b/p}}{p} e^{-\frac{1}{2}|\mathbf{s} - \frac{1}{2}\hat{\mathbf{u}}\hat{\mathbf{x}}|^2} e^{-\frac{1}{2}p^2 + \frac{1}{2}\hat{\mathbf{u}}p_x - \frac{1}{8}\hat{\mathbf{u}}^2}}{2 \iint \frac{d^3 p d^3 s}{(2\pi)^3} \frac{e^{-b/p}}{p} e^{-\frac{1}{2}s^2} e^{-\frac{1}{2}p^2}}, \quad (9)$$

where $s \doteq (\mathbf{w} + \mathbf{w}')/\sqrt{2}v_{\text{th}}$ and $\hat{\mathbf{u}} \doteq \sqrt{2}u_0/v_{\text{th}}$. Assuming $\hat{\mathbf{u}} \lesssim 1$, evaluating (9) to leading order in b yields

$$\Phi \sim \frac{1}{2} + \frac{e^{-\frac{1}{12}\hat{\mathbf{u}}^2} \sinh\left(\frac{1}{2}\hat{\mathbf{u}}b^{1/3}\right)}{\hat{\mathbf{u}}b^{1/3}} \quad (10)$$

By (8), $\langle \sigma v \rangle$ is a strongly decreasing function of b (so an increasing function of temperature) in reactor-relevant regimes. However, by (10), Φ is an increasing function of b . Therefore, while fusion reactivity is largest at high temperature, the fractional enhancement is largest at low temperature. Additionally, the flow speed u_0 corresponding to a fixed $\hat{\mathbf{u}}$ is smaller at low temperature. For these reasons, a promising application of strongly sheared flow is to ‘jump-start’ a fusion burn in warm fuel.

Numerical results – To improve on the analytical estimate in (10), we solved (4) numerically in steady state. Because collisions with ions and electrons are of comparable importance for fast ions, we adopted a BGK operator with collision frequency $\nu = \nu_{\text{ii}} + \nu_{\text{ie}}$. The ion-ion collision frequency ν_{ii} was given by the same model as above and the ion-electron collision frequency was a constant $\nu_{\text{ie}} = \nu_0 \sqrt{m_e/\bar{m}}$ where m_e , m_D , and m_T are the electron, deuterium, and tritium masses respectively and $\bar{m} \doteq (m_D + m_T)/2$. An equimolar DT plasma was assumed and velocities normalized to $\bar{v}_{\text{th}} \doteq \sqrt{T/\bar{m}}$. The background was a Maxwellian with uniform temperature and with stationary flow profile

$$\mathbf{u}(z) = \frac{u_0}{2} \left(1 - \tanh\left(\frac{z}{L}\right)\right) \hat{\mathbf{x}} \quad (11)$$

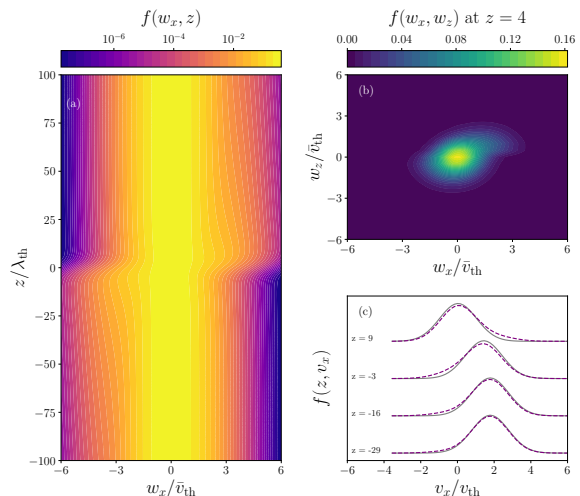


Figure 2: Distribution function for a $u_0 = 2v_{\text{th}}$, $L = 5\lambda_{\text{th}}$ layer. (a) $f(z, w_x)$ showing a jump in peculiar velocity near $z = 0$. (b) $f(w_x, w_z)$ showing the anisotropic distribution of fast particles. (c) $f(z, v_x)$ (purple, dotted) compared to $f_M(z, v_x)$ (grey); cf. Fig. 1.

for constant flow velocity u_0 and gradient length scale L .

Viewed in the $z - w_x$ plane (Fig. 2a), the perturbation to f appears as ‘wings’ near $z = 0$, where particles coming from the other side of the shear layer have not yet ‘caught up’ to the local flow velocity. This phenomenon affects all particles, but it persists over a much longer distance for fast particles. In the $w_x - w_z$ plane (Fig. 2b), the perturbation appears as a lobe of higher phase-space density at $w_x, w_z > 0$; this fast-ion population is responsible for the enhancement in reactivity.

From these distributions, reactivity was calculated using the cross-section formulas of Bosch & Hale [44] for the $\text{D}(\text{d}, \text{n})^3\text{He}$ and $\text{T}(\text{d}, \text{n})^4\text{He}$ reactions (Fig. 3). The enhancements (Φ_{DD} and Φ_{DT} respectively) peak just outside the transition layer, but actually dip within the layer because the maximum difference in flow velocity is not as large there as in the outer regions. As anticipated by (10), the enhancement factor is larger at low temperature [45]. For the most extreme conditions tested, Φ_{DT} reaches 2.4 at its peak, a dramatic increase in fusion rate over a region tens of λ_{th} in width. For equivalent conditions, Φ_{DD} is larger than Φ_{DT} due to a leveling off of the DT cross section at high energy. This is consistent with experiments finding a lower than expected DT:DD yield ratio [38]. The reactivity enhancement is an inherently kinetic effect. To illustrate this, moments of f were computed at each z location for one flow profile ($u_0 = \bar{v}_{\text{th}}$, $L = 5\lambda_{\text{th}}$) and Maxwellians were generated with the same moments. Reactivities for these distributions are shown in grey in Fig. 3, demonstrating that much of the enhancement is not attributable to bulk heat-

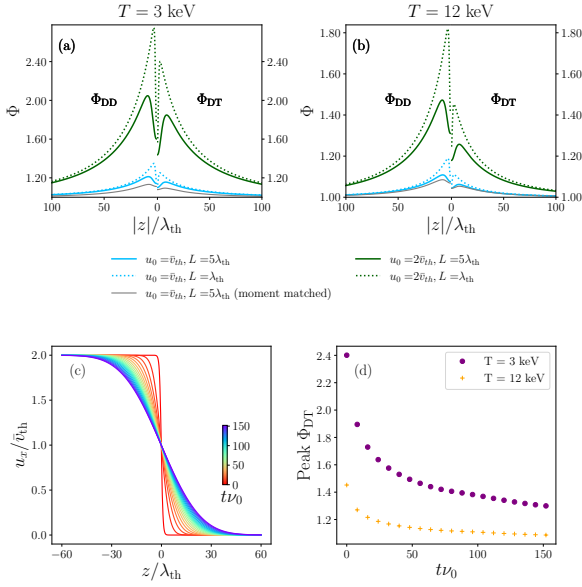


Figure 3: Top: reactivity enhancement at (a) $T = 3$ keV and (b) $T = 12$ keV. The left half of each panel shows Φ_{DD} and the right shows Φ_{DT} . Bottom: (c) flow relaxation and (d) peak Φ_{DT} at each time step.

ing alone.

The flow profile described by (11) is subject to rapid viscous dissipation when $L \sim \lambda_{th}$. To assess the effect of viscosity on reactivity, we performed kinetic simulations in Gkeyll [46] using as initial conditions (11) with $u_0 = 2v_{th}$ and $L = \lambda_{th}$. Fig. 3 shows the flow profile at later times (c) and the height of the peak of the Φ_{DT} profile at each time (d). Reactivity drops quickly at first, but begins to level off at later times; $(\Phi_{DT} - 1)$ drops to about one sixth of its original value in 150 collision times. For the parameters discussed below, this is about 30 ps, meaning that the enhancement is significant for a large fraction of the burn duration [47]. This analysis neglects hydrodynamic instabilities, which may transiently increase Φ , much as instabilities aggravate the Knudsen-layer reactivity reduction [20].

Neutron spectra – Fusion product spectroscopy is a crucial diagnostic tool, yielding direct information about reactant distributions. Each point near a shearing region produces a distinct neutron spectrum. For a layer with $u_0 = 2v_{th}$ and $L = \lambda_{mfp}$ at $T = 3$ keV and $T = 12$ keV, Fig. 4, shows moments from the $D(d,n)^3He$ and $T(d,n)^4He$ neutron spectra at each point along a path from $z = -500\lambda_{th}$ to $z = 0$ (solid curves). Crilly *et al.* [16] have shown that any superposition of spectra produced by Maxwellian reactants lies below the ‘Maxwellian locus,’ which is displayed for stationary and flowing distributions. Without kinetic effects, spectra for a sheared system lie on the dotted lines connecting the stationary and flowing Maxwellian loci. The solid curves

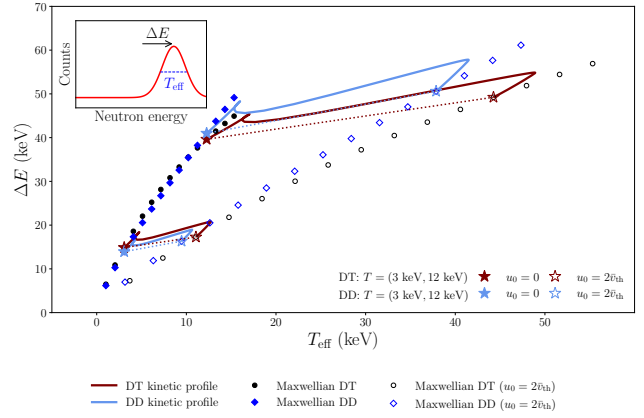


Figure 4: Inset: spectral moments for DT and DD reactions. Markers: Maxwellian loci [16] for stationary (filled) and flowing (hollow) DT (circles) and DD (diamonds). Stars: Maxwellians at $T = 3$ keV and $T = 12$ keV, marked for clarity. Curves: kinetic spectra near a $u_0 = 2v_{th}$, $L = \lambda_{mfp}$ shear layer.

lie above this line, demonstrating the importance of kinetic physics. For the shear layer considered here, the spectrum does not pass above the stationary Maxwellian locus, but it does exhibit a larger ΔE than can be explained by flowing Maxwellians at the temperatures considered. Notably, T_{eff} is larger for the DT reaction than for the DD reaction. This matches the puzzling experimental observation that the temperature inferred from DT neutrons is often higher than that inferred from DD neutrons [20, 38].

Discussion – Why has flow shear not previously been considered alongside other kinetic modifications to reactivity? The answer lies, at least in part, in its multidimensional nature, involving at least one spatial dimension and two velocity dimensions (see Fig. 2), as well as a velocity-dependent collision frequency. Simplifications made in many kinetic simulations, such as one-dimensional velocity space, spherical symmetry, and constant collision frequency, obscure these features [4, 6, 12, 18, 48]. Although previously overlooked, flow shear is estimated to have a moderate effect in pre-ignition phases of experiments at the National Ignition Facility (NIF).

Based on high-resolution simulations [49, 50] of National Ignition Campaign (NIC) experiment N120321, we consider a region with ion density $n \sim 10^{25} \text{ cm}^{-3}$ and temperature $T \sim 2.5$ keV. Simulations with physical viscosity indicate that gradients are weak in much of the hotspot, but are strong in a few regions, such around the fill-tube perturbation (cf. Fig. 9 of [49] and Fig. 7 of [50]). Estimating in these regions $u \sim 1.6\bar{v}_{th}$ and $L \sim 20\lambda_{th}$ yields a peak DT reactivity enhancement of 22% ($\Phi_{DT} \approx 1.22$, while $\Phi_{DD} \approx 1.29$). The peak is about $5 \mu\text{m}$ in width. Taking the hotspot radius to be

$R \sim 40 \mu\text{m}$ and estimating the total area of the shear layers to be half of the hotspot surface area (although folded deep within the hotspot), the volume-averaged DT reactivity enhancement is a more modest 4%. Ignited NIF targets exhibit conditions comparable to N120321 during the shock phase, but high-temperature conditions later in compression produce a smaller effect [47, 51, 52]. At the other extreme, sub-ignition experiments [1, 5, 18, 53] have explored strongly kinetic regimes, relevant to early phases of compression, in which Φ is of order unity (see Fig. 3).

Sheared flow can spark a fusion burn even when the volume-averaged enhancement is small. A localized jet of fuel at high velocity with a sharp boundary would trigger a local increase in fusion rate, which can be designed, like ‘striking a match,’ to ignite the rest of the fuel. This process is similar to other fast-ignition schemes [54, 55], but with the advantage of not requiring collisional heating of the ions to ignition temperatures, which can be both inefficient [56, 57] and prohibitively slow [58]. In the sudden viscous dissipation effect, compression of a turbulent plasma leads first to growth in the turbulent kinetic energy and then to rapid dissipation [36]. This phenomenon has been suggested for reducing radiative losses during compression, with the turbulent energy thermalizing immediately before bang time [37]. The results in this Letter render this scenario even more attractive by showing that significant fusion can occur before thermalization, which in turn increases the viscous dissipation rate.

The basic physical mechanism described in this Letter is not specific to ICF, although ICF is particularly promising for its generation of high-Mach number flows on short length scales. The effect is likewise not specific to unmagnetized plasma. Because classical cross-field transport in magnetized plasma is determined by the gyroradius rather than the mean free path, energetic particles in magnetized plasmas do not have as large an advantage over their thermal cousins. Sheared flow is therefore likely to have a smaller, but possibly still important, effect on the reactivity of magnetized plasmas.

Acknowledgments – This work was supported by the Center for Magnetic Acceleration, Compression, and Heating (MACH), part of the U.S. DOE-NNSA Stewardship Science Academic Alliances Program under Cooperative Agreement DE-NA0004148.

* hfetsch@princeton.edu

- [1] K. Molvig, N. M. Hoffman, B. J. Albright, E. M. Nelson, and R. B. Webster, *Physical Review Letters* **109**, 095001 (2012).
- [2] B. J. Albright, K. Molvig, C.-K. Huang, A. N. Simakov, E. S. Dodd, N. M. Hoffman, G. Kagan, and P. F. Schmit, *Physics of Plasmas* **20**, 122705 (2013).
- [3] S. Davidovits and N. J. Fisch, *Physics of Plasmas* **21**, 092114 (2014).
- [4] M. Rosenberg, H. Rinderknecht, N. Hoffman, P. Amendt, S. Atzeni, A. Zylstra, C. Li, F. Séguin, H. Sio, M. G. Johnson, *et al.*, *Physical Review Letters* **112**, 185001 (2014).
- [5] H. G. Rinderknecht, M. Rosenberg, C. Li, N. Hoffman, G. Kagan, A. Zylstra, H. Sio, J. Frenje, M. Gatu Johnson, F. Séguin, *et al.*, *Physical Review Letters* **114**, 025001 (2015).
- [6] A. Inglebert, B. Canaud, and O. Larroche, *Europhysics Letters* **107**, 65003 (2014).
- [7] H. Sio, O. Larroche, S. Atzeni, N. V. Kabadi, J. A. Frenje, M. Gatu Johnson, C. Stoeckl, C. K. Li, C. J. Forrest, V. Glebov, *et al.*, *Physics of Plasmas* **26**, 072703 (2019).
- [8] J. D. Sadler, Y. Lu, B. Spiers, M. W. Mayr, A. Savin, R. H. W. Wang, R. Aboushelbaya, K. Glize, R. Bingham, H. Li, K. A. Flippo, and P. A. Norreys, *Physical Review E* **100**, 033206 (2019).
- [9] B. E. Peigney, O. Larroche, and V. Tikhonchuk, *Physics of Plasmas* **21**, 122709 (2014).
- [10] C. J. McDevitt, X.-Z. Tang, and Z. Guo, *Physics of Plasmas* **24**, 112702 (2017).
- [11] X.-Z. Tang, T. Elder, C. J. McDevitt, and Z. Guo, *Europhysics Letters* **123**, 65002 (2018).
- [12] O. M. Mannion, W. T. Taitano, B. D. Appelbe, A. J. Crilly, C. J. Forrest, V. Y. Glebov, J. P. Knauer, P. W. McKenty, Z. L. Mohamed, C. Stoeckl, *et al.*, *Physical Review E* **108**, 035201 (2023).
- [13] B. Du, D. Kang, S. Zou, C. Liu, L. Deng, F. Ge, Z. Dai, H. Cai, and S. Zhu, *Physics of Plasmas* **31**, 012706 (2024).
- [14] D. S. Clark, D. E. Hinkel, D. C. Eder, O. S. Jones, S. W. Haan, B. A. Hammel, M. M. Marinak, J. L. Milovich, H. F. Robey, L. J. Suter, and R. P. J. Town, *Physics of Plasmas* **20**, 056318 (2013).
- [15] H. G. Rinderknecht, P. A. Amendt, M. J. Rosenberg, C. K. Li, J. A. Frenje, M. G. Johnson, H. Sio, F. H. Séguin, R. D. Petrasso, and A. B. o. Zylstra, *Nuclear Fusion* **57**, 066014 (2017).
- [16] A. J. Crilly, B. D. Appelbe, O. M. Mannion, W. Taitano, E. P. Hartouni, A. S. Moore, M. Gatu-Johnson, and J. P. Chittenden, *Nuclear Fusion* **62**, 126015 (2022).
- [17] E. P. Hartouni, A. S. Moore, A. J. Crilly, B. D. Appelbe, P. A. Amendt, K. L. Baker, D. T. Casey, D. S. Clark, T. Döppner, M. J. Eckart, *et al.*, *Nature Physics* **19**, 72–77 (2023).
- [18] H. G. Rinderknecht, P. A. Amendt, S. C. Wilks, and G. Collins, *Plasma Physics and Controlled Fusion* **60**, 064001 (2018).
- [19] O. Larroche, H. G. Rinderknecht, and M. J. Rosenberg, *Physical Review E* **98**, 031201 (2018).
- [20] G. Kagan, D. Svyatskiy, H. Rinderknecht, M. Rosenberg, A. Zylstra, C.-K. Huang, and C. McDevitt, *Physical Review Letters* **115**, 105002 (2015).
- [21] M. J. Rosenberg, F. H. Séguin, P. A. Amendt, S. Atzeni, H. G. Rinderknecht, N. M. Hoffman, A. B. Zylstra, C. K. Li, H. Sio, M. Gatu Johnson, *et al.*, *Physics of Plasmas* **22**, 062702 (2015).
- [22] B. M. Haines, *Physics of Plasmas* **31**, 050501 (2024).
- [23] C. R. Weber, D. S. Clark, A. W. Cook, L. E. Busby, and H. F. Robey, *Physical Review E* **89**, 053106 (2014).
- [24] T. J. Murphy, *Physics of Plasmas* **21**, 072701 (2014).
- [25] J. L. Giuliani, J. W. Thornhill, E. Kroupp, D. Osin, Y. Maron, A. Dasgupta, J. P. Apruzese, A. L. Velikovich,

- Y. K. Chong, A. Starobinets, *et al.*, *Physics of Plasmas* **21**, 031209 (2014).
- [26] E. Kroupp, D. Osin, A. Starobinets, V. Fisher, V. Bernshtam, L. Weingarten, Y. Maron, I. Uschmann, E. Förster, A. Fisher, M. E. Cuneo, C. Deeney, and J. L. Giuliani, *Physical Review Letters* **107**, 105001 (2011).
- [27] Y. Maron, *Physics of Plasmas* **27**, 060901 (2020).
- [28] V. A. Thomas and R. J. Kares, *Physical Review Letters* **109**, 075004 (2012).
- [29] D. S. Clark, S. W. Haan, A. W. Cook, M. J. Edwards, B. A. Hammel, J. M. Koning, and M. M. Marinak, *Physics of Plasmas* **18**, 082701 (2011).
- [30] B. M. Haines, T. J. Murphy, R. E. Olson, Y. Kim, B. J. Albright, B. Appelbe, T. H. Day, M. A. Gunderson, C. E. Hamilton, T. Morrow, and B. M. Patterson, *Physics of Plasmas* **30**, 072705 (2023).
- [31] T. J. Murphy, B. J. Albright, M. R. Douglas, T. Cardenas, J. H. Cooley, T. H. Day, N. A. Denissen, R. A. Gore, M. A. Gunderson, J. R. Haack, *et al.*, *High Energy Density Physics* **38**, 100929 (2021).
- [32] J. E. Ralph, J. S. Ross, A. B. Zylstra, A. L. Kritcher, H. F. Robey, C. V. Young, O. A. Hurricane, A. Pak, D. A. Callahan, K. L. Baker, *et al.*, *Nature Communications* **15**, 2975 (2024).
- [33] A. Pak, L. Divol, C. R. Weber, L. F. B. Hopkins, D. S. Clark, E. L. Dewald, D. N. Fittinghoff, V. Geppert-Kleinrath, M. Hohenberger, S. L. Pape, *et al.*, *Physical Review Letters* (2020).
- [34] T. Ma, P. K. Patel, N. Izumi, P. T. Springer, M. H. Key, L. J. Atherton, L. R. Benedetti, D. K. Bradley, D. A. Callahan, P. M. Celliers, *et al.*, *Physical Review Letters* **111**, 085004 (2013).
- [35] R. J. Mason, R. C. Kirkpatrick, and R. J. Faehl, *Physics of Plasmas* **21**, 022705 (2014).
- [36] S. Davidovits and N. J. Fisch, *Physical Review Letters* **116**, 105004 (2016).
- [37] S. Davidovits and N. J. Fisch, *Physics of Plasmas* **25**, 042703 (2018).
- [38] M. G. Johnson, J. P. Knauer, C. J. Cerjan, M. J. Eckart, G. P. Grim, E. P. Hartouni, R. Hatarik, J. D. Kilkenny, D. H. Munro, D. B. Sayre, B. K. Spears, R. M. Bionta, E. J. Bond, J. A. Caggiano, D. Callahan, D. T. Casey, T. Doppner, J. A. Frenje, V. Y. Glebov, O. Hurricane, A. Kritcher, S. LePape, T. Ma, A. Mackinnon, N. Meezan, P. Patel, R. D. Petrasso, J. E. Ralph, P. T. Springer, and C. B. Yeaman, *PHYSICAL REVIEW E* (2016).
- [39] D. R. Mikkelsen, *Nuclear Fusion* **29**, 1113 (1989).
- [40] K. K. Kirov, E. Belonohy, C. D. Challis, J. Eriksson, D. Frigione, L. Garzotti, L. Giacomelli, J. Hobirk, A. Kappatou, D. Keeling, *et al.*, *Nuclear Fusion* **61**, 046017 (2021).
- [41] E. J. Kolmes, M. E. Mlodik, and N. J. Fisch, *Physics of Plasmas* **28**, 052107 (2021).
- [42] H. Xie, M. Tan, D. Luo, Z. Li, and B. Liu, *Plasma Physics and Controlled Fusion* **65**, 055019 (2023).
- [43] T. H. Rider, *Physics of Plasmas* **4**, 1039–1046 (1997).
- [44] H.-S. Bosch and G. M. Hale, *Nuclear Fusion* **32**, 611 (1992).
- [45] Note that the length and velocity scales in each plot depend on temperature. Therefore, the peak is about sixteen times wider, in absolute units, in the $T = 12$ keV plot.
- [46] A. Hakim, M. Francisquez, J. Juno, and G. W. Hammett, *Journal of Plasma Physics* **86**, 905860403 (2020).
- [47] A. L. Kritcher, A. B. Zylstra, C. R. Weber, O. A. Hurricane, D. A. Callahan, D. S. Clark, L. Divol, D. E. Hinkel, K. Humbird, O. Jones, *et al.*, *Physical Review E* **109**, 025204 (2024).
- [48] N. M. Hoffman, G. B. Zimmerman, K. Molvig, H. G. Rinderknecht, M. J. Rosenberg, B. J. Albright, A. N. Simakov, H. Sio, A. B. Zylstra, M. Gatu Johnson, *et al.*, *Physics of Plasmas* **22**, 052707 (2015).
- [49] D. S. Clark, M. M. Marinak, C. R. Weber, D. C. Eder, S. W. Haan, B. A. Hammel, D. E. Hinkel, O. S. Jones, J. L. Milovich, P. K. Patel, *et al.*, *Physics of Plasmas* **22**, 022703 (2015).
- [50] C. R. Weber, D. S. Clark, A. W. Cook, D. C. Eder, S. W. Haan, B. A. Hammel, D. E. Hinkel, O. S. Jones, M. M. Marinak, J. L. Milovich, *et al.*, *Physics of Plasmas* **22**, 032702 (2015).
- [51] M. J. Rosenberg, A. B. Zylstra, F. H. Séguin, H. G. Rinderknecht, J. A. Frenje, M. Gatu Johnson, H. Sio, C. J. Waugh, N. Sinenian, C. K. Li, *et al.*, *Physics of Plasmas* **21**, 122712 (2014).
- [52] O. A. Hurricane, D. A. Callahan, D. T. Casey, P. M. Celliers, C. Cerjan, E. L. Dewald, T. R. Dittrich, T. Döppner, D. E. Hinkel, L. F. B. Hopkins, *et al.*, *Nature* **506**, 343–348 (2014).
- [53] T. Yabe and K. A. Tanaka, *Laser and Particle Beams* **7**, 259–265 (1989).
- [54] M. Tabak, J. Hammer, M. E. Glinsky, W. L. Kruer, S. C. Wilks, J. Woodworth, E. M. Campbell, M. D. Perry, and R. J. Mason, *Physics of Plasmas* **1**, 1626–1634 (1994).
- [55] M. Tabak, D. Hinkel, S. Atzeni, E. M. Campbell, and K. Tanaka, *Fusion Science and Technology* **49**, 254–277 (2006).
- [56] S. Atzeni, *Physics of Plasmas* **6**, 3316–3326 (1999).
- [57] M. Tabak, D. S. Clark, S. P. Hatchett, M. H. Key, B. F. Lasinski, R. A. Snavely, S. C. Wilks, R. P. J. Town, R. Stephens, E. M. Campbell, *et al.*, *Physics of Plasmas* **12**, 057305 (2005).
- [58] H. Fetsch and N. J. Fisch, *Physical Review E* **108**, 045206 (2023).